



## Research Article

Nusrat Sharmin\*, Mohammad S. Hasan, Md. Towhidul Islam, Chengheng Pang, Fu Gu, Andrew J. Parsons, and Ifty Ahmed

# Effect of dissolution rate and subsequent ion release on cytocompatibility properties of borophosphate glasses

<https://doi.org/10.1515/bglass-2019-0008>

Received Oct 02, 2019; revised Nov 02, 2019; accepted Nov 06, 2019

**Abstract:** Present work explores the relationship between the composition, dissolution rate, ion release and cytocompatibility of a series of borophosphate glasses. While, the base glass was selected to be 40mol%P<sub>2</sub>O<sub>5</sub>-16mol%CaO-24mol%MgO-20mol%Na<sub>2</sub>O, three B<sub>2</sub>O<sub>3</sub> modified glass compositions were formulated by replacing Na<sub>2</sub>O with 1, 5 and 10 mol% B<sub>2</sub>O<sub>3</sub>. Ion release study was conducted using inductively coupled plasma atomic emission spectroscopy (ICP-AES). The thermal scans of the glasses as determined by differential scanning calorimetry (DSC) revealed an increment in the thermal properties with increasing B<sub>2</sub>O<sub>3</sub> content in the glasses. On the other hand, the dissolution rate of the glasses decreased with increasing B<sub>2</sub>O<sub>3</sub> content. To identify the effect of boron ion release on the cytocompatibility properties of the glasses, MG63 cells were cultured on the surface of the glass discs. The in vitro cell culture study suggested that glasses with 5 mol% B<sub>2</sub>O<sub>3</sub> (P40B5) showed better cell proliferation and metabolic activity as compares to the glasses with 10 mol% (P40B10) or with no B<sub>2</sub>O<sub>3</sub> (P40B0). The confocal laser scanning microscopy (CLSM) images of live/dead stained MG63 cells attached to the surface of the glasses also revealed that the number of dead cells attached to P40B5 glasses were significantly lower than both P40B0 and P40B10 glasses.

**Keywords:** Phosphate based glasses, ion release, glass dissolution, cytocompatibility, live/dead cells staining

## 1 Introduction

Degradable implants are attracting huge interest these days for different biomedical applications particularly for treating large bone defect as temporary implant materials. This increasing demand is mainly due to the fact that bone defects above a critical size cannot be repaired by the self-healing of bone tissue [1, 2]. Therefore, degradable osteoconductive device or scaffold is required to support the regeneration of new tissue. Phosphate based glasses (PBGs) are one of the most promising candidates in this respect as these glasses can completely dissolve in aqueous medium and the dissolution rate can be altered via altering the glass composition [3–6]. Moreover, these PBGs can be doped with different modifier oxide in order to achieve a controlled dissolution rate and associated ion release [7–9]. Several researchers have reported the effect of different modifier oxide addition on the structural, dissolution, thermal, ion release and cytocompatibility properties of PBGs [10–14].

The degradation process of PBGs takes place by ionic exchange of soluble ions which is strongly depended on the glass composition [15]. It has been reported that the cytocompatibility of PBGs are strongly dependent on the dissolution rate and associated ion release. The release of different ions in therapeutic concentrations can help to stimulate the regenerative system to restore body tissue [3]. On the other hand, release of certain ions in excess amount may impose negative impact on human body. As for ex-

\*Corresponding Author: **Nusrat Sharmin:** Department of Chemical and Environmental Engineering, University of Nottingham Ningbo China, China; Ningbo Nottingham International Academy for the Marine Economy and Technology, University of Nottingham Ningbo China, Ningbo, 315100, China; Ningbo Nottingham New Materials Institute, University of Nottingham Ningbo China, Ningbo, 315100, China; Email: nusrat.sharmin@nottingham.edu.cn, nusrat\_sharmin27@yahoo.com

**Mohammad S. Hasan, Md. Towhidul Islam, Ifty Ahmed:** Advanced Materials Research Group, Healthcare Technologies, Faculty of Engineering, University of Nottingham, Nottingham, NG7 2RD, United Kingdom

**Chengheng Pang, Fu Gu:** Department of Chemical and Environmental Engineering, University of Nottingham Ningbo China, China  
**Andrew J. Parsons:** Composites Research Group, Healthcare Technologies, Faculty of Engineering, University of Nottingham, NG7 2RD, United Kingdom



ample, release of  $Mg^{2+}$  has been reported to have positive influence on the bone formation and bone growth [5, 16]. Therefore, it is very important to carefully engineer the glass formulation in order to achieve the appropriate therapeutic effect.

It has been reported that the addition of different amount of boron oxide to bioactive glasses has significant effect on the glass structure, glass dissolution rate, thermal properties, processing parameters, biocompatibility and cytotoxicity [17]. Addition of  $B_2O_3$  to PBGs can increase the chain length of the main glass structure by becoming a part of main glass network and as such can make the fibre drawing process easier [18]. However, it was also reported that the addition of higher amount of  $B_2O_3$  (more than 5 mol%) may impose less positive effect on the cell proliferation and cell metabolic activity [9]. Therefore, it is very important to understand the effect of different amount of boron ion release on positive or negative cellular response.

It is well known that boron is a beneficial bioactive element for wound healing and can stimulate the bone healing process [10]. It has been reported that optimal level of boron is required in human body for calcium metabolism and boron deficiency can have detrimental effect on bone formation and maintenance [19]. Moreover, boron is also needed to prevent excessive bone loss in post-menopausal women and older men [20].

A good understanding on the interplay between glass structure, degradation kinetics, ion release and cytocompatibility provides flexibility for the development of scaffolds with highly specific cellular response. The effect of  $B_2O_3$  addition on the structure of PBGs with similar formulation has already been reported in a previous publication [18]. In this current study four different PBGs formulations were designed to investigate the effect of boron ion ( $B^{3+}$ ) release on the cytocompatibility properties of the glasses. The initial aim of the study was to establish a relationship between the dissolution rate, ion release and cytocompatibility of PBGs with phosphate contents fixed at 40mol% containing  $B_2O_3$ . The main aim of the present work was to explore how the different composition of different  $B_2O_3$  containing glasses influence the *in vivo* cell attachment, metabolic activity and proliferation. The effect of increasing  $B_2O_3$  addition on the thermal and dissolution properties of the glasses were also evaluated.

## 2 Materials and methodology

### 2.1 Glass preparation

Glass compositions under investigation in this current study were prepared using melt quenching method, where appropriate amount of precursors were weighed, mixed properly and melted in a platinum crucible at  $1200^\circ C$  for 2 hours. Before melting the mixed glass, precursors were pre-heated at  $350^\circ C$  for half an hour to remove any trace of moisture. The molten glass was then casted in a graphite mould (9mm\*100mm) which was preheated at  $450^\circ C$  and then allowed to cool down approximately at a rate of  $0.5^\circ C/min$  to room temperature. The  $P_2O_5$ , CaO and MgO content in all four glasses were fixed to 40, 16 and 24 mol%, respectively. While, 1, 5 and 10 mol%  $B_2O_3$  was added at the expense of  $Na_2O$ . The glasses containing 0, 1, 5 and 10 mol%  $B_2O_3$  has been coded as P40B0, P40B1, P40B5 and P40B10 throughout the study, respectively. The precursors that were used for glass preparations are phosphorus pentoxide ( $P_2O_5$ , Sigma Aldrich, UK, >98%), sodium dihydrogen phosphate ( $NaH_2PO_4$ , Sigma Aldrich, UK,  $\geq 99\%$ ), calcium hydrogen phosphate ( $CaHPO_4$ , Sigma Aldrich, UK, 98-105%), magnesium hydrogen phosphate trihydrate ( $MgHPO_4 \cdot 3H_2O$ , Sigma Aldrich, UK,  $\geq 98\%$ ) and boron oxide ( $B_2O_3$ , Sigma Aldrich, UK,  $\geq 99\%$ ).

### 2.2 Powder X-ray diffraction analysis

The powder X-ray diffraction analysis was conducted on all glass samples before dissolution study to confirm the amorphous nature of the glasses. A Bruker D500 X-ray diffractometer with Ni-filtered  $CuK\alpha$ -radiation ( $\lambda=0.15418$  nm), operated at 40 kV and 40 mA was used for the analysis. The experiment was conducted at room temperature. The angular range  $2\theta$  for each scan was from  $15^\circ$  to  $100^\circ$  with a step size of  $0.02^\circ$  and a step time of 0.5 s.

### 2.3 Thermal analysis

The thermal analysis of the glasses was conducted using a differential scanning calorimeter (TA Instruments SDT Q600, UK). The glasses were grounded to fine powder and was heated from room temperature to  $520^\circ C$  under flowing argon gas at a rate of  $20^\circ C \text{ min}^{-1}$  to determine the glass transition temperature ( $T_g$ ). Once the  $T_g$  was determined then the glass samples was heated from room temperature to a temperature which is  $T_g + 20^\circ C$ , held there isothermally for 15 min, cool down to room temperature

and then heated again to 1100°C. The whole experiment was conducted under flowing argon gas and the heating and cooling rate used was 20°C min<sup>-1</sup> and 10°C min<sup>-1</sup>, respectively. This repeated heating cycle was used to introduce a known thermal history for all the glasses under investigation. The glass transition ( $T_g$ ), onset of crystallisation ( $T_x$ ), peak crystallisation ( $T_c$ ), melting ( $T_m$ ) and liquidus temperatures ( $T_l$ ) was determined from the second ramping cycle.

## 2.4 Dissolution studies

The dissolution study was conducted on glass discs with a 9mm diameter and 5 mm thickness. Three glass discs from each formulation was immersed in glass vials containing 30ml of phosphate buffer solution (PBS). Then the glass vials were placed in an incubator at 37°C. At designated time point the glass discs were taken out from the vials, dried and the area and the mass of the discs were measured. The study was conducted for 60 day and at each time point fresh PBS solution was added to the discs. The rate of mass loss (%) was calculated according to the following equation:

$$\text{Mass Loss (\%)} = \frac{M_0 - M_t}{M_0}$$

Where  $M_0$  is the initial mass (g) and  $M_t$  is the mass at time  $t$ . The mass loss per area data were plotted as weight loss per unit area against time. The slope of this graph gave the dissolution rate in terms of kg m<sup>-2</sup> s<sup>-1</sup>.

## 2.5 Compositional analysis and ion release studies

The compositional and ion release analyses of the glass samples were conducted using inductively coupled plasma atomic emission spectroscopy (ICP-AES, Perkin Elmer Optima 7300, MA, USA). Standard solution containing B, P, Na<sup>+</sup>, Ca<sup>2+</sup>, Fe<sup>3+</sup> and Mg<sup>2+</sup> was prepared before each cycle of measurement to obtain calibration curves. The concentrations of the calibration solution was maintained at 1, 10 and 100 ppm in 2% HNO<sub>3</sub> in DI water. Standard sample concentrations were measured periodically to ensure accuracy of the calibration curves. Each analysis was repeated for three times. The ICP-AES instrument was calibrated using NIST traceable aqueous standards. The sample solutions were analysed against their calibration curves.

For compositional analysis each glass formulation was ground in to powder using a rotating ball mill and 0.1g

of powder from each formulation was digested in 5ml 70% HCl until a clear solution was obtained. The solution was then diluted 100 times using 2% HNO<sub>3</sub> in DI water prior to ICP-AES analysis. For ion release studies the 9 mm glass rods were cut in to 5 mm thick glass discs. The glass discs were then immersed in 30 ml ultra-pure (Milili-Q) water kept in glass vials. The temperature of the glass vials containing the glass discs were maintained at 37°C. At day 1, 7, 14 and 21, 0.1mL of supernatant liquor from glass formulation was diluted with 9.9ml 3% nitric acid and analysed to determine sodium, boron, calcium and magnesium ion release from the glass samples.

## 2.6 Cell culture

The cell culture study was conducted in a similar way as mentioned in a previous publication [9]. Briefly, the metabolic activity and proliferation of the MG63 cells cultured on the glass samples were assessed using alamar blue assay and DNA (Hoechst 33258) assay, respectively. The MG63 cells (human osteosarcoma) was collected from the European Collection of Cell Cultures (ECACC). The cells were cultured in complete Dulbecco's Modified Eagle Medium (CDMEM) consisting of DMEM supplemented with 10% foetal calf serum (FCS), 2% HEPES buffer, 2% penicillin/streptomycin, 1% glutamine, 1% nonessential amino acids (Gibco Invitrogen, UK), and 0.85 mM of ascorbic acid (Sigma Aldrich, UK) in 75 cm<sup>3</sup> flasks at 37°C in a humidified atmosphere with 5% CO<sub>2</sub>. The seeding concentration of the MG63 cells cultured on the glass samples were 60,000 cells/cm<sup>2</sup>. The glass discs were thoroughly sterilised and washed with PBS solution prior to cell culture studies. The cell culture study was conducted for 7 days. In order to observe the morphology of the cells cultured on the glass samples were taken out from the cell culture flasks, carefully washed with warm PBS (37°C). Then the cells were fixed with 3% glutaraldehyde in 0.1M Nacacodylate buffer for 30 minutes, 7% sucrose solution for 30 minutes and 1% osmium tetroxide in PBS for 45 minutes. Afterwards the samples were dehydrated using 20, 30, 40, 50, 60, 70, 80, 90, 96 and 100% ethanol flowed by drying using hexamethyldisilazine (HMDS). Finally, the dried samples were sputter coated in platinum and the morphology of the cells cultured on glass samples were observed using a Philips XL30 scanning electron microscope operated at 20 kV.

**Table 1:** The thermal characteristics ( $T_x$ ,  $T_c$ ,  $T_m$ ,  $T_L$ ) for P40B0, P40B1, P40B5 and P40B10 glasses.

Glass batch composition /mol%	$T_{c,ons}$ / °C	$T_c$ / °C	$T_m$ / °C	$T_L$ / °C
P40B0	503.6±0.6	539.7 ±0.6 626.5 ±0.3	754.8±0.2	788.1±0.3
P40B1	511.4±1.0	546.0 ±0.6 659.6 ±0.5	751.2±0.5	806.1±0.6
P40B5	539.7±0.9	586.1 ±0.3 699.3 ±0.6	780.8±0.7	909±0.5
P40B10	587.6±0.7	626.9 ±0.7 743.2 ±0.5	873.6±0.1	940.6±0.4

## 2.7 Cell viability and live/dead staining

The number of live and dead cells present on the glass samples was quantified using a BioVision's Live/Dead Cell Viability Assay Kit. This kit provides a two-color fluorescence method that is based on the simultaneous determination of live and dead cells using two different dyes. In order to determine the number of live or dead cells present 2  $\mu$ l of Live Cell staining dye was mixed with 1  $\mu$ l of dead cell staining dye in 1 ml of assay buffer. 0.5 ml of the dye solution was added in per well in 24 well dish followed by incubation at 37°C for 15 min. Live cell dye used in this kit can easily penetrates intact, live cells and intracellular esterase hydrolyzes the dye to produce a hydrophilic, strongly fluorescent compound that is retained in the cell cytoplasm which can be measured at Ex/Em = 485/530 nm. On the other hand, the dead cell dye can only enter damaged cell membranes and undergoes a 40-fold enhancement of fluorescence upon binding to nucleic acid, thereby producing a bright red fluorescence (Ex/Em = 495/635 nm). The assessment of cell viability in three dimensions was performed using confocal laser scanning microscopy (CLSM, Bio-Rad, USA).

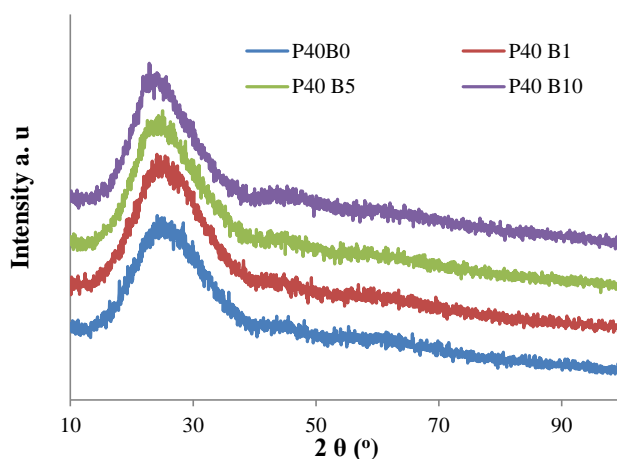
## 2.8 Statistical analyses

Average values and standard deviation were computed, and statistical analysis was performed using the Prism software package (version 8.3.0, GraphPad Software, San Diego California USA, www.graphpad.com). Two-way analysis of variance (ANOVA) was calculated with the bonferroni post-test to compare the significance of change in one factor with time. The error bars presented represent standard deviation with  $n = 3$ .

## 3 Results

### 3.1 Powder X-ray diffraction analysis

Figure 1 represents the XRD traces of the P40 glass series investigated. No sharp crystalline peak was observed in the XRD traces of the glasses. Therefore, the presence of only a single broad peak observed between 20° and 40° in the XRD curves of the glass samples confirmed the amorphous nature of the glasses.

**Figure 1:** Powder X-ray diffraction pattern for P40B0, P40B1, P40B5 and P40B10 glasses.

### 3.2 Thermal analysis

The effect of  $B_2O_3$  addition on the thermal properties of the glasses are presented in Figure 2. The glass transition ( $T_g$ ), onset of crystallisation ( $T_x$ ), peak crystallisation ( $T_c$ ), melting ( $T_m$ ) and liquidus temperatures ( $T_L$ ) increased with increasing  $B_2O_3$  content from 0 to 10 mol%. The  $T_g$  value

for P40B0 glasses (glass composition with 0 mol%  $B_2O_3$ ) was  $\sim 434^\circ C$ , which increased to  $\sim 463^\circ C$  and  $\sim 500^\circ C$  for P40B5 (glass compositions with 5 mol%  $B_2O_3$ ) and P40B10 (glass compositions with 10 mol%  $B_2O_3$ ) glasses, respectively. However, an increase of only  $\sim 5^\circ C$  in the  $T_g$  values was observed as 1 mol%  $B_2O_3$  was added to P40B0 glasses. Similar increasing trend was also observed for onset of crystallisation ( $T_x$ ), peak crystallisation ( $T_c$ ), melting ( $T_m$ ) and liquidus temperatures ( $T_l$ ) for 1 mol%  $B_2O_3$  addition. Two crystalline peaks ( $T_{c1}$  and  $T_{c2}$ ) were observed for all four glasses under investigation. In addition, the intensity of the crystalline peaks decreased and also the peaks became less defined as the  $B_2O_3$  content in the glasses increased from 0 to 10 mol%.

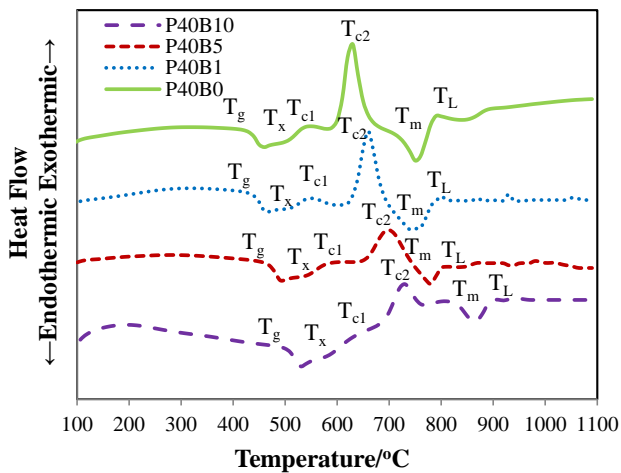


Figure 2: Thermal scans (DSC) for the P40B0, P40B1, P40B5 and P40B10 glasses.

### 3.3 Glass solubility

Figure 3 and Figure 4 represent the mass loss in percentage and the degradation rate of the glasses investigated, respectively. As seen from Figure 3, there was no significant difference ( $p < 0.05$ ) between the mass loss percentage of P40B0 and P40B1 glasses. P40B10 showed the lowest mass loss percentage as compared to all four glass formulations investigated. The mass loss percentage of P40B5 glasses was higher than P40B10 glasses, however still significantly lower than both P40B0 and P40B1 glasses. After 60 days of immersion in PBS the mass loss percentage of P40B0, P40B1, P40B5 and P40B10 was  $\sim 2.9\%$ ,  $\sim 2.9\%$ ,  $\sim 1.75\%$  and  $\sim 1.25\%$ , respectively. The dissolution rate of the glasses was calculated considering the change in dimension of the glass discs along with mass loss with time

which followed the same trend as the mass loss percentage. No statistical significant difference was observed between the degradation rate of P40B0 and P40B1 glasses. After 60 days of immersion, the dissolution rate for the P40B0 glasses was  $2.04 \times 10^{-8}$ , whilst the P40B5 and P40B10 glasses showed a dissolution rate of  $8.84 \times 10^{-9}$  and  $8.64 \times 10^{-9} \text{ kg m}^{-2} \text{ s}^{-1}$ , respectively.

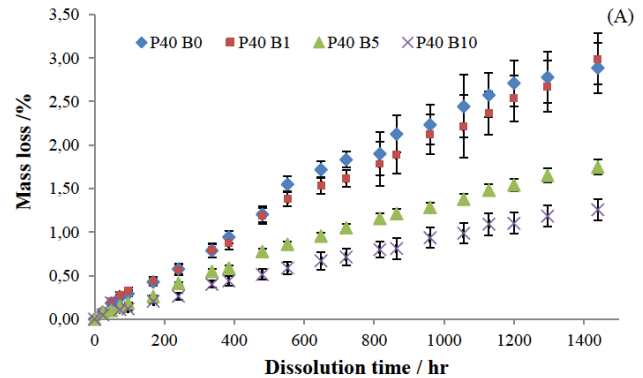


Figure 3: Plot of Mass loss (%) of the P40B0, P40B1, P40B5 and P40B10 glasses in PBS at  $37^\circ C$  for 60 days.

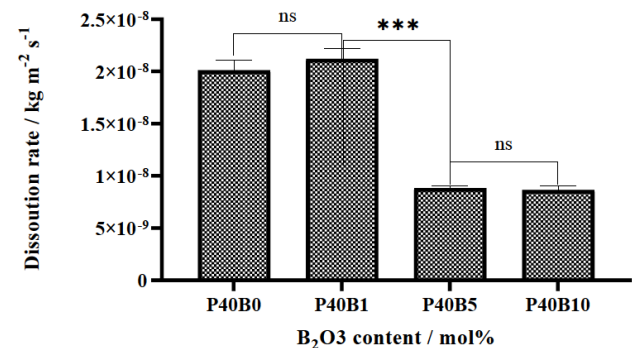


Figure 4: Dissolution rate values obtained for P40B0, P40B1, P40B5 and P40B10 glasses.

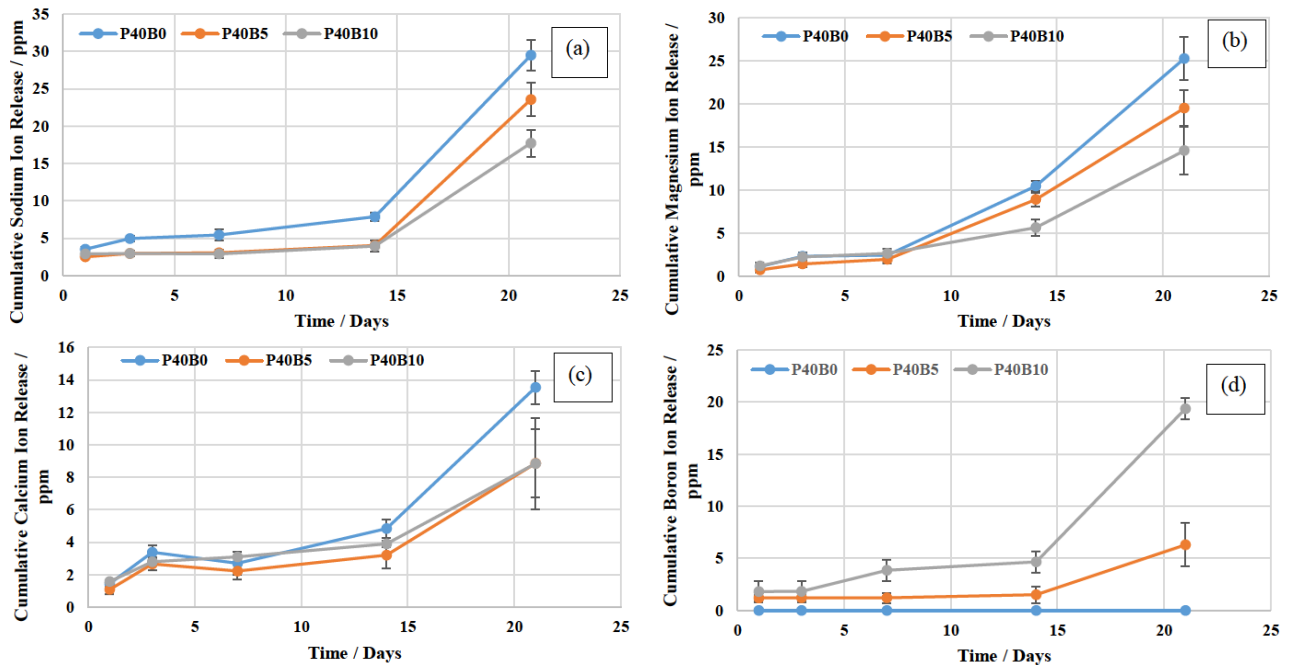
### 3.4 Ion release studies

The composition of the glasses as determined by ICP-AES is presented in Table 2.

Figure 5(a-d) shows the sodium ( $Na^+$ ), calcium ( $Ca^{2+}$ ), magnesium ( $Mg^{2+}$ ) and boron ( $B^{3+}$ ) ion release profiles of the glasses investigated as a function of time. As seen from Figure 5(a), at all time points P40B0 glass formulation showed the highest  $Na^+$  release. At day 21,  $\sim 21 \text{ ppm}$   $Na^+$  release was observed for P40B0 glass formulation. P40B5

**Table 2:** Compositions of the glasses determined by ICP-AES.

Glass batch composition / mol%	P <sub>2</sub> O <sub>5</sub> / mol%	CaO / mol%	Na <sub>2</sub> O / mol%	MgO / mol%	B <sub>2</sub> O <sub>3</sub> / mol%
P40					
P40B0	36.7±0.10	17.7±0.01	25.1±0.17	22.5±0.14	-
P40B1	37.8±0.05	16.7±0.05	20.1±0.15	24.5±0.15	0.8±0.01
P40B5	37.5±0.06	17.7±0.06	17.6±0.12	25.9±0.18	5.1±0.21
P40B10	38.0±0.08	19.1±0.10	10.7±0.05	27.8±0.24	8.7±0.14

**Figure 5:** Cumulative sodium (a), magnesium (b), calcium (c) and boron (d) ion release from P40B0, P40B5 and P40B10 glasses.

and P40B10 glass formulation showed similar ion release profile up to day 14. At day 21, ~23 ppm and ~18 ppm Na<sup>+</sup> release was observed from P40B5 and P40B10 glass formulation, respectively. Figure 5(b) and 5(c) represents the Mg<sup>2+</sup> and Ca<sup>2+</sup> release profiles of the glasses investigated. Up to day 7, there was no significant difference in Mg<sup>2+</sup> and Ca<sup>2+</sup> release for all glass samples. At day 14, all three glass samples showed similar Ca<sup>2+</sup> release profile. At day 14 P40B10 glass formulation showed ~7ppm Mg<sup>2+</sup> ion release, whereas, both P40B5 and P40B0 glasses showed ~4 ppm Mg<sup>2+</sup> ion release profiles. For P40B0 glass ~25ppm and ~14ppm Mg<sup>2+</sup> and Ca<sup>2+</sup> ion release was observed at day 21 which was significantly higher than both P40B5 and P40B10 glasses. Figure 3(d) shows the B<sup>3+</sup> release profiles for P40B5 and P40B10 glass formulations. There was no significant difference in B<sup>3+</sup> release was observed between P40B5 and P40B10 glasses up to day 3. At all other points (day 7, 14 and 21), P40B10 glasses showed significantly

higher B<sup>3+</sup> release as compared to P40B5 glasses. At day 7, 14 and 21 the B<sup>3+</sup> release from P40B5 and P40B10 glasses were ~1.2ppm, ~1.5ppm, ~6.3ppm and ~3.8ppm, ~4.6ppm, ~19.0ppm, respectively.

### 3.5 Cytocompatibility studies

The cell culture study was conducted for 7 days and time points used were day 1, 3, 5 and 7. The metabolic activity of the MG63 cells cultured on the glass samples and TCP (Tissue Culture Plastic) internal control are presented in Figure 6. At day 1, there was no significant difference ( $p > 0.05$ ) between the metabolic activity of the cells cultured on the glass samples and the TCP. From Day 3, TCP showed elevated metabolic activity as compared to the glass samples. At day 5, there was no significant difference ( $p > 0.05$ ) between the metabolic activity of the cells cultured on P40B0

and P40B10 glasses. However, the cells cultured on P40B5 glasses showed higher metabolic activity as compared to both P40B0 and P40B10 glasses as day 5. At day 7, the lowest metabolic activity was observed for the cell cultured on P40B10 glasses, whereas, the cells cultured on P40B5 glasses showed the highest metabolic activity.

Figure 7 represents the cell proliferation of MG63 osteosarcoma, as measured by the DNA concentration over 7 days of cell culture. As seen from the figure, all three glass samples and TCP showed continuous proliferation over the entire cell culture period. TCP showed the highest cell proliferation as compared with the glass samples as day 5 and day 7 of cell culture. No significant difference in the DNA concentration was observed among the glass samples at day 1 and day 3. However, at day 5 and day 7 the DNA concentrations of the cells cultured on P40B5 glasses were significantly higher than those on P40B0 and P40B10 glasses.

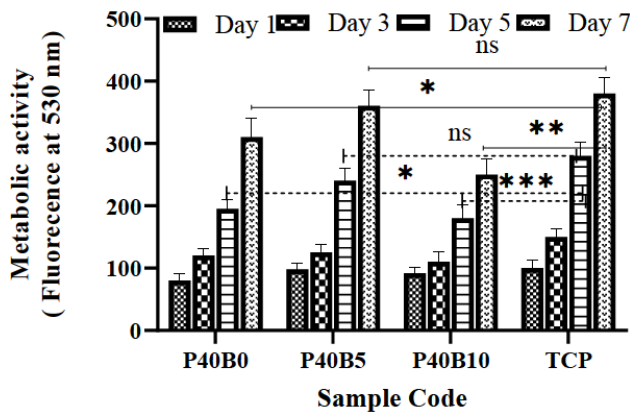


**Figure 6:** Metabolic activity of MG63 cells, measured by the alamar blue assay, cultured on glass samples: error bars represent the standard deviation for  $n=3$ . The solid lines represent the statistical difference between samples at day 7 and the dotted lines represent the statistical difference between samples at day 5.

### 3.6 Cell morphology

Figure 8 shows the SEM images of the MG63 cells attached on the surface of the glass samples after 1, 5 and 7 days of culture. At day 1, there was fewer cells attached to the glass samples as compared to day 5 and day 7. The glass surfaces were covered with dense multi layered cells after 5 and 7 days of culture. However, no visible difference in the cell morphology among different glass samples were observed at any particular time point.

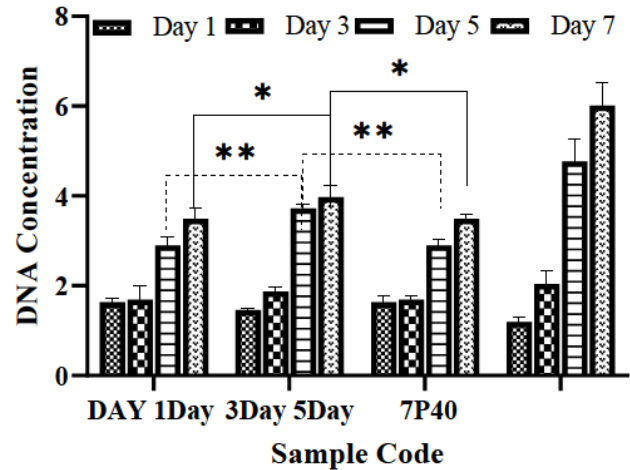


**Figure 7:** Cell proliferation of MG63 osteosarcoma, as measured by the DNA (Hoechst 33258) assay, cultured on glass samples. Error bar represents standard deviation for  $n=3$ . The solid lines represent the statistical difference between samples at day 7 and the dotted lines represent the statistical difference between samples at day 5.

In order to further explore the relationship between the effects of amount of borate ion release or the dissolution rate with the cytocompatibility of the glasses a live/dead cell assay was conducted. Figure 9 and 10 shows confocal laser scanning microscopy (CLSM) images of live/dead stained MG63 cells attached to the surface of the tested glass compositions after 1, 5 and 7 days of culture. At day 5 and day 7, cells cultured on P40B0, P40B5 and P40B10 glasses showed almost similar staining pattern consisting of a confluent monolayer of green fluorescent live cells. Very sparse number of red fluorescent dead cells was observed at day 1 on all glass samples. P40B5 glass maintained the same pattern in terms of visible red fluorescent dead cells even at day 5 and day 7. However, there were a noticeably higher number of red fluorescent dead cells observed on P40B5 and P40B10 glasses at day 5 and day 7. Although qualitative in nature, the *in vitro* live/dead assay provides additional evidence that the P40B5 glasses showed better cellular response as compared to P40B0 and P40B10 glasses.

## 4 Discussion

It is very important to control the rate of degradation and associated ion release of any biomaterials as the uncontrolled degradation and ion release can result in loss of their mechanical integrity and metal contamination in human body, respectively [5].

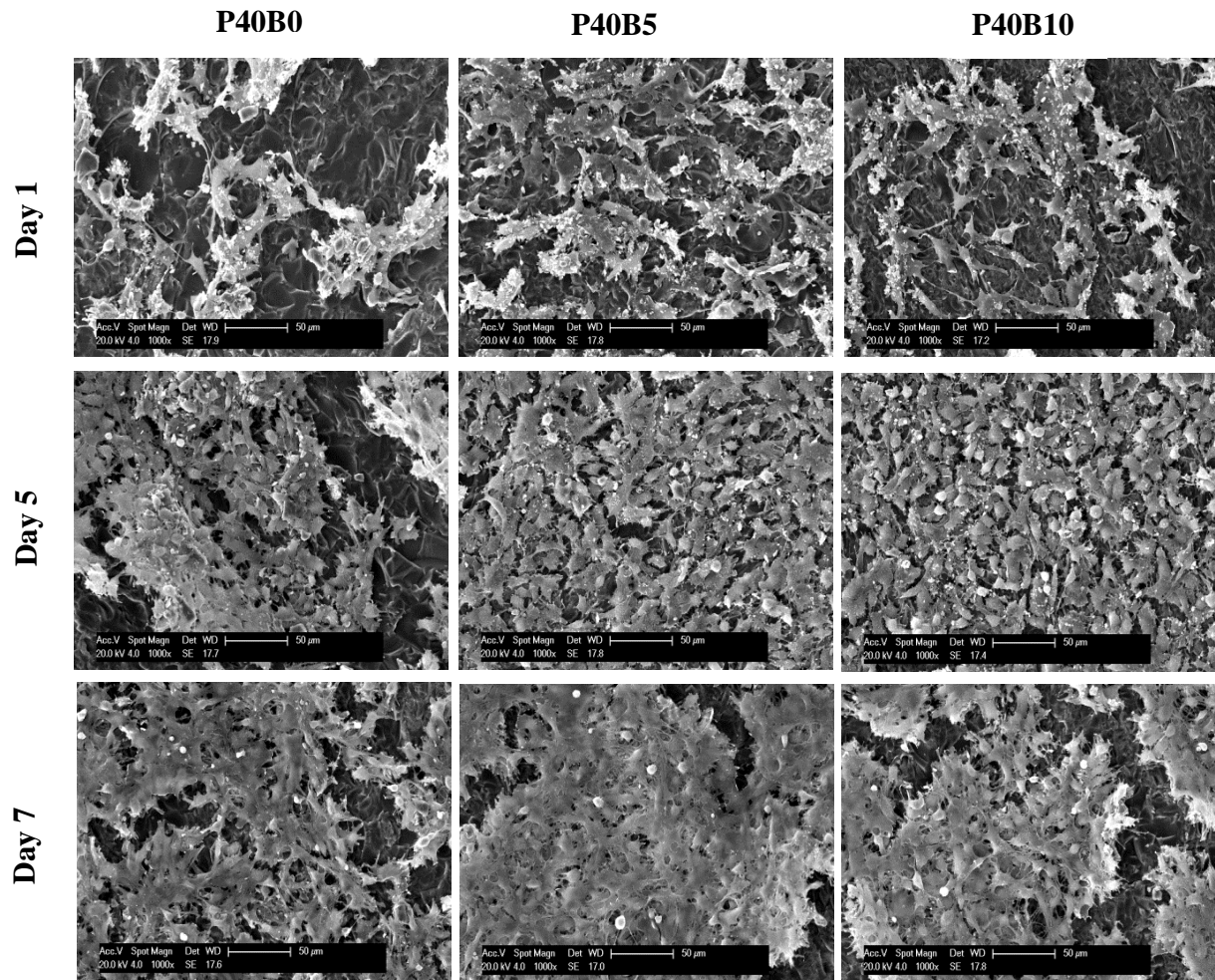


**Figure 8:** SEM images of the MG63 cells cultured on P40B0, P40B5 and P40B10 glasses after 1, 5 and 7 days of culture.

The amorphous nature of the glass compositions studied was confirmed via XRD before the thermal analysis and dissolution studies. In our current study  $\text{Na}_2\text{O}$  was replaced with 1, 5 and 10 mol%  $\text{B}_2\text{O}_3$ . Figure 4 represents that the dissolution rate of P40B5 and P40B10 glasses were ~56% lower than that of P40B0 glasses. Therefore, it was clear that addition of 5 and 10 mol%  $\text{B}_2\text{O}_3$  significantly reduced the dissolution rate. The degradation of phosphate based glasses takes place by where hydrogen ions interchange with cations to form  $\text{P-OH}^-$  and subsequent disentanglement of the polymer like glass structure via hydrolysis [21]. The reduction in dissolution rate with  $\text{B}_2\text{O}_3$  addition could be due to the formation of more hydration resistant P-O-B bonds. Carta *et al.* studied the structure of borophosphate glasses and they reported the presence of P-O-B bonds in the glass structure [22]. They also reported that increasing amount of  $\text{B}_2\text{O}_3$  in the glasses increased the level of cross-linking between phosphate and borate units. These increased cross linking in phosphate glass

structure could also potentially increase the glass durability. Maserra *et al.* reported that the addition of as small as 1.25 mol%  $\text{B}_2\text{O}_3$  to PBGs can significantly decrease the dissolution rate [23]. They also suggested that addition of  $\text{B}_2\text{O}_3$  can led to the formation of more hydration resistant P-O-B bonds and thus increase the chemical durability. However, in our study similar level of  $\text{B}_2\text{O}_3$  substitution did not show any significant effect on dissolution rate. It could be due to fact that Maserra *et al.* substituted  $\text{P}_2\text{O}_5$  for  $\text{B}_2\text{O}_3$ , whereas in our study  $\text{B}_2\text{O}_3$  was substituted for  $\text{Na}_2\text{O}$  and hence showed less pronounced effect on dissolution rate at such level. Donald *et al.* studied the influence of  $\text{B}_2\text{O}_3$  addition on the sodium aluminium glasses and suggested that quite small additions of  $\text{B}_2\text{O}_3$  can provide considerable benefit in improving the thermal properties and durability of phosphate glasses [24]. They suggested that the improvement in durability could be due to the formation of durable  $\text{BPO}_4$  groups.



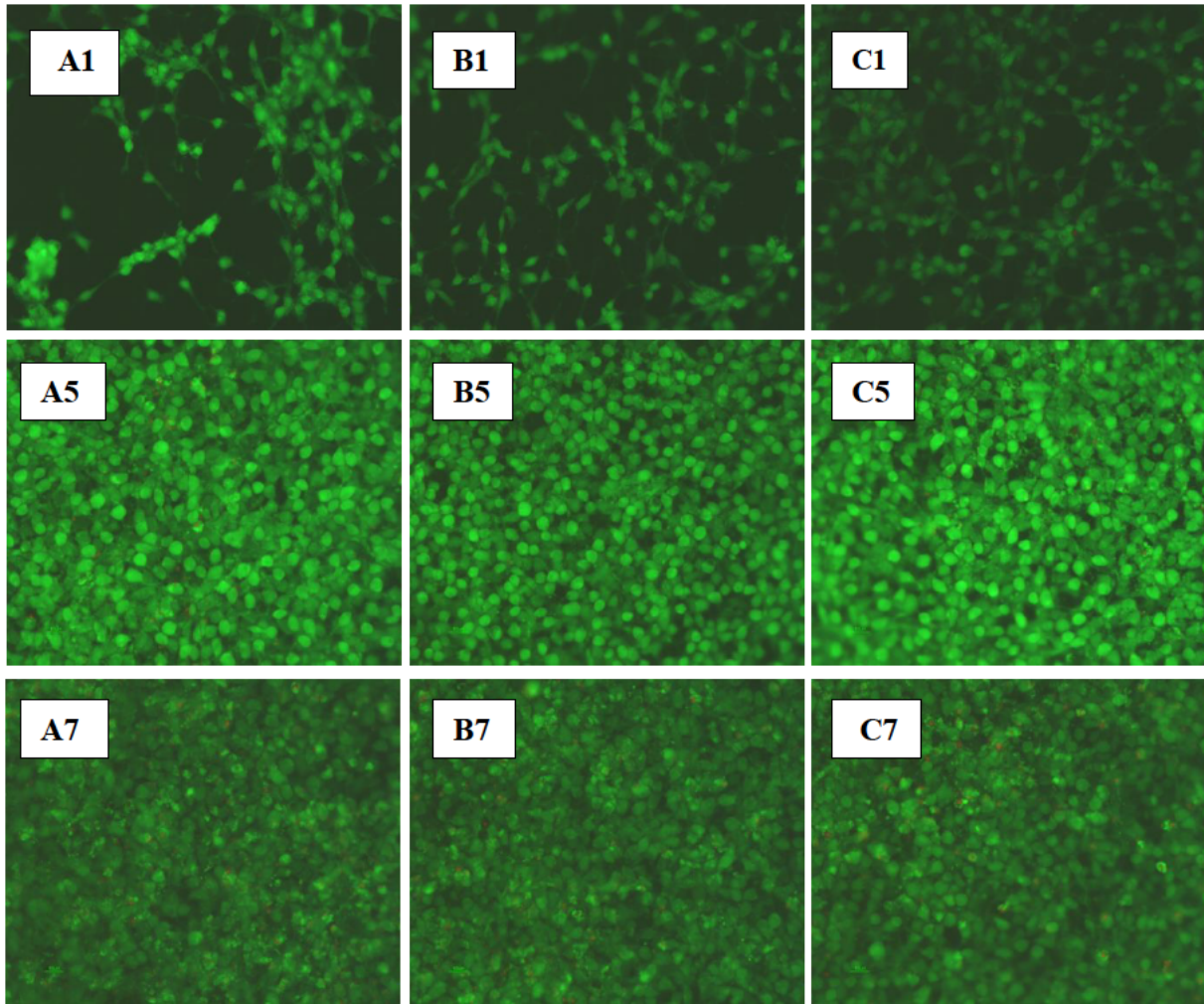


**Figure 9:** CLSM images showing the viability of MG63 cells cultured on the surface of different glass compositions. Live cells are stained green. A, B and C represents P40B0, P40B5 and P40B10 glasses. 1, 5 and 7 represents the corresponding days of culture.

The DSC scans of the glasses suggested that the glass transition ( $T_g$ ), onset of crystallisation ( $T_x$ ), peak crystallisation ( $T_c$ ), melting ( $T_m$ ) and liquidus temperatures ( $T_l$ ) increased with increasing  $B_2O_3$  content in the glass series. However, the dissolution rate of the glasses decreased with increasing  $B_2O_3$  addition. Similar trends in thermal properties and dissolution rate with increasing  $B_2O_3$  content was reported in a previous publication where phosphate content was fixed to 45 and 50 mol% [9]. It was suggested that increasing glass transition temperatures and other thermal properties with boron oxide addition at the cost of sodium oxide was due to the higher B-O bond strength as compared to Na-O bond strength [9]. The thermal properties composition containing two glass former oxides depends on the connectivity of the associated glass forming units [25, 26]. This connectivity can be defined in term of the average number of bridging oxygens. In our

study, replacing  $Na_2O$  with  $B_2O_3$  can decrease the number of non-bridging oxygens which can also increase the glass transition temperature. Joseph *et al.* reported that phosphate based glasses containing Ba showed higher glass transition temperature as compared to glasses containing similar amount of Cs [27]. They suggested that the higher glass transition temperature of Ba containing glasses were due to the better glass network connectivity of the glasses which was introduced due to the greater cationic field strength of Ba as compared to Cs.

It is worth to mention that the glass transition temperature of the glasses with 40 mol%  $P_2O_5$  studied in our current study are lower than the glasses with 45 and 50 mol% with similar composition. Phosphate glasses with higher phosphate content (50 mol%  $P_2O_5$ ) are supposed to be more dominant in long chains or rings structures (*i.e.*  $Q^2$  species) as compared to glasses with lower  $P_2O_5$  con-

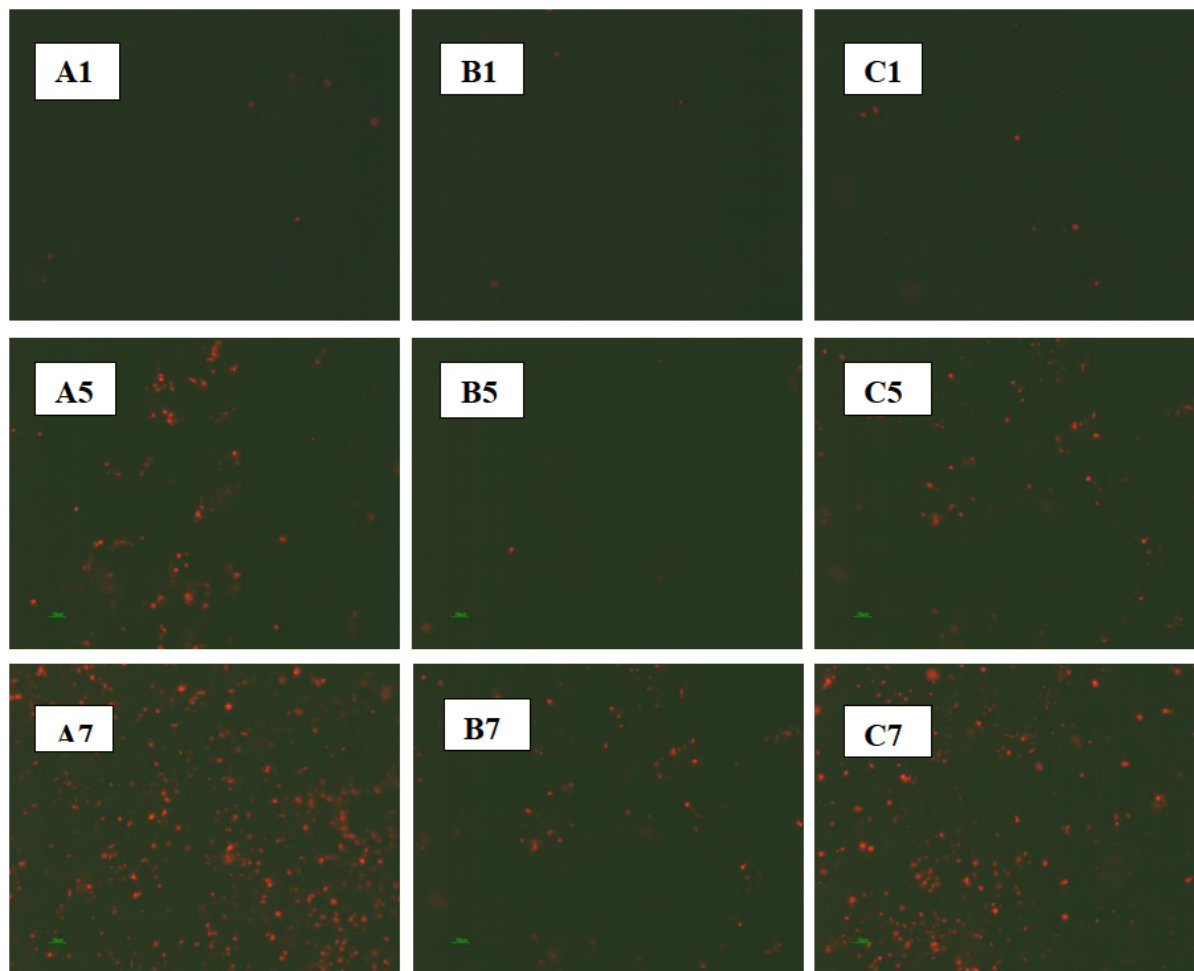


**Figure 10:** CLSM images showing the viability of MG63 cells cultured on the surface of different glass compositions. Dead cells are stained red. A, B and C represents P40B0, P40B5 and P40B10 glasses. 1, 5 and 7 represents the corresponding days of culture.

tent which is responsible for higher  $T_g$  values [4, 28]. Reducing the  $P_2O_5$  content from 50 to 40 mol% will introduce shorter chain  $Q^1$  species in the glass structure which would account for the lower  $T_g$  values for glasses with 40 mol%  $P_2O_5$ . It has also been suggested that the addition of boron oxide could alter the dimensionality of the phosphate network via the formation of long chain  $Q^2$  species rather than  $Q^0$  or  $Q^1$  units [18, 29, 30]. Therefore, addition of  $B_2O_3$  to the phosphate based glasses could potentially increase the chain length of the main glass structure which in turn would increase the glass transition temperature and other associated thermal properties of the glasses.

As, there was not a significant difference between 0 and 1 mol%  $B_2O_3$  containing glasses in terms of thermal and dissolution properties, only 0, 5 and 10 mol%  $B_2O_3$  containing glasses were considered for ion release and cell culture studies.

As seen from Figure 5(a), lower  $Na^+$  release was observed from the glasses containing 5 mol% (P40B5) and 10 mol%  $B_2O_3$  (P40B10) as compared to the glasses with no  $B_2O_3$  (P40B0). This behaviour could be attributed to the fact that in P40B5 and P40B10 glasses were prepared by adding 5 and 10 mol%  $B_2O_3$  to P40B0 glasses at the expense of  $Na_2O$ . Therefore, the replacement of  $Na_2O$  with  $B_2O_3$  in P40B5 and P40B10 glasses is reducing the available amount of  $Na^+$  which is eventually reducing the  $Na^+$  release from the glasses as compared to P40B0. Moreover, the degradation rate of both P40B5 and P40B10 glasses are much lower than P40B0 glasses which could also contribute to the lower  $Na^+$  release from these glasses. Abou Neel *et al.* conducted an ion release study on the phosphate glass fibres containing  $Fe_2O_3$  and the reported that glasses with higher amount of  $Fe_2O_3$  showed lower  $Na^+$  release [7]. They suggested that this reduced  $Na^+$  release was due to the replacement of  $Na_2O$  with  $Fe_2O_3$  and thus re-

ducing the available  $\text{Na}^+$  in the glass and also due to the increased durability of the glasses with increasing  $\text{Fe}_2\text{O}_3$  content. Although, the amount of  $\text{MgO}$  and  $\text{CaO}$  was same, the glass compositions under investigation showed different  $\text{Mg}^{2+}$  and  $\text{Ca}^{2+}$  ion release profile particularly after 7 days of degradation.

The P40B0 glasses showed highest  $\text{Mg}^{2+}$  and  $\text{Ca}^{2+}$  release at day 14 and day 21. This confirmed the fact that the ion release profile of the glasses is affected by the degradation rate of the corresponding glasses. Therefore, as discussed above addition of increasing amount of  $\text{B}_2\text{O}_3$  to the glasses is increasing the durability of the glasses via increasing the compactness of the glass structure which is eventually reducing the amount of  $\text{Mg}^{2+}$  and  $\text{Ca}^{2+}$  release of P40B5 and P40B10 glasses as compared to P40B0 glasses.

Figure 5(d) shows the  $\text{B}^{3+}$  release profile for P40B5 and P40B10 glasses. As seen from figure 3 the mass loss percentage of P40B10 glasses with time were significantly lower than P40B5 glasses. However, the  $\text{B}^{3+}$  release from P40B10 glasses were significantly higher than that for P40B5 glasses. Therefore, similar as  $\text{Na}^+$  release profile of the glasses, higher amount of  $\text{B}^{3+}$  release from P40B10 glasses could be attributed to the presence of higher amount of  $\text{B}_2\text{O}_3$  as compared to P40B5 glasses.

An ideal biomaterial should provide the appropriate platforms for cell attachment, proliferation and differentiation to be effectively used for bone tissue engineering [6, 31]. It has been reported by several scientists that the ionic product of degradation alongside with the degradation rate has huge effect on cell proliferation and gene expression–differentiation [8, 9, 32]. The degradation rate is important as a stable surface is required for the cells to attach and proliferate as any material with high degradation rate cannot provide a stable surface for the cell growth [17]. On the other hand, ionic products released during the degradation can change the pH of the cell culture medium resulting an undesired cell response [8]. In our current study, P40B5 glasses showed better cell metabolic activity and proliferation as compared to both P40B0 and P40B10 glasses. Moreover, as seen from Figure 10, the number of dead cells attached on the surface of P40B5 glasses after 7 days of culture were significantly lower than those of P40B0 and P40B10 glasses. However, no significant difference was observed between the cell metabolic activity and proliferation between P40B0 and P40B10 glasses.

As is evidenced from our degradation studies the degradation rate of P40B10 glasses were significantly lower than P40B0 glasses and there was no statistically significant difference between the dissolution rate of P40B10 and P40B5 glasses. Therefore, the degradation rate of the

P40B10 glasses were not responsible for the less positive cellular positive response of the glasses. As seen from Figure 5(d), the boron ion release from P40B10 glasses after 3 days of degradation was significantly higher than P40B5 glasses. A release of 1.20 ppm of  $\text{B}^{3+}$  was observed from P40B5 glasses, whereas the P40B10 glasses released 4.0 ppm  $\text{B}^{3+}$  at day 7.

Vrouwenvelder *et al.* studied the incorporation of 5 wt%  $\text{B}_2\text{O}_3$  in the 45S5 Bioglass® network and reported that the glass discs showed compact morphology, normal morphology and moderate osteoblast expression [33]. However, Fu *et al.* studied the in vitro performance of the borate based bioactive glasses for potential bone repair applications [34]. They reported that the threshold concentration of the borate ion released from the glasses without any negative effect on the proliferation of bone marrow stromal cells were ~0.65 mM. Brown *et al.* also suggested that high  $\text{B}_2\text{O}_3$  content in the glasses can inhibit the cell proliferation and this effect could be avoided if the borate ion concentration in the cell culture medium could be kept below a certain threshold level [35]. They reported that this effect could be achieved by using a borosilicate glass composition in which less than 1/3 of the  $\text{SiO}_2$  in 45S5 glass was replaced by  $\text{B}_2\text{O}_3$ . The extracts from the glasses supported the cell proliferation and function up to this concentration. The release of phosphate ions and borate ions could change the pH of the solution due to the formation of phosphoric acid and boric acid, respectively [36]. Uo *et al.* studied the relationship between composition, dissolution rate and cytotoxicity of  $\text{P}_2\text{O}_5$ -CaO- $\text{Na}_2\text{O}$  glasses [37]. They reported that the glass compositions containing higher  $\text{P}_2\text{O}_5$  content show low toxicity and the toxicity increases with increasing phosphate content. They suggested that the pH of the solution changed to acidic as the  $\text{P}_2\text{O}_5$  content in the glasses increased from 50 to 60 mol% which was responsible for the higher cytotoxicity. Elena *et al.* also suggested that high levels of phosphorus and boron can impose a detrimental effect on biocompatibility properties of glasses [38]. Rajkumar *et al.* also reported similar effect of pH variation on the cell growth of human osteoblast like cell lines [39]. Therefore, the combined release of  $\text{B}^{3+}$  ions and  $(\text{PO}_4)^{3-}$  ions from the glasses results in an increase in pH which could alter the cell metabolic and ALP activities. In our current study P40B5 glasses better cellular activity in terms of cell metabolic activity, proliferation and the number of dead cell present on the glass surface as compared to P40B10 glasses.

It could be concluded that the complexity of glass formulations can significantly affect the dissolution behaviour, ion release and in turn the in vitro bioactivity. Variations in glass formulations can completely change

the dissolution and cytocompatibility properties of the glasses as the rate of different ion release can enhance or inhibit the cell attachment, viability and proliferation. Therefore, boron oxide modified glasses have prospective future as bone tissue engineering scaffolds as long as the glass formulations are carefully engineered.

## 5 Summary

Phosphate based glasses in the system of 40mol%P<sub>2</sub>O<sub>5</sub>-16mol%CaO-24mol%MgO-20mol%Na<sub>2</sub>O was selected as base glass for this study. 1, 5 and 10 mol% B<sub>2</sub>O<sub>3</sub> was added to the glass system at the expense of Na<sub>2</sub>O. The glass transition temperature and other thermal properties of the glasses increased with increasing B<sub>2</sub>O<sub>3</sub> content. On the other hand, the glass dissolution rate decreased with increasing B<sub>2</sub>O<sub>3</sub> content. However, there was not a significant difference between 0 and 1 mol% B<sub>2</sub>O<sub>3</sub> containing glasses in terms of thermal and dissolution properties. Therefore, only 0, 5 and 10 mol% B<sub>2</sub>O<sub>3</sub> containing glasses were considered for ion release and cell culture studies. The ion release studies revealed that the P40B10 glasses showed maximum B<sup>3+</sup> ion release. While, P40B0 glasses showed highest Na<sup>+</sup> release. The 5 mol% B<sub>2</sub>O<sub>3</sub> containing glasses showed better cellular response as compared to glasses with 0 mol% B<sub>2</sub>O<sub>3</sub> and 10 mol% B<sub>2</sub>O<sub>3</sub> containing the glasses. The negative cellular response from P40B0 glasses were due to higher dissolution rate, whilst an excessive amount of boron ion release was responsible for the lower cell metabolic activity and proliferation of the cells cultured on P40B10 glasses. In conclusion, boron oxide modified phosphate based glasses have prospective future as bone tissue engineering scaffolds as long as the amount of boron ion release from the glasses is kept under a threshold limit which is 4 ppm for our glass series.

**Acknowledgement:** This work is financially supported by the Industrial Technology Innovation and Industrialization of Science and Technology Project, China (2014A35001-2).

**Ethical approval:** The conducted research is not related to either human or animals use.

**Conflict of Interests:** The authors declare no conflict of interest regarding the publication of this paper.

## References

- [1] Ciraldo F.E., Boccardi E., Melli V., Westhauser F., Boccaccini A.R., Tackling bioactive glass excessive in vitro bioreactivity: Preconditioning approaches for cell culture tests, *Acta Biomater.*, 2018, 75, 3-10.
- [2] Perez R.A., Seo S.-J., Won J.-E., Lee E.-J., Jang J.-H., Knowles J.C., et al., Therapeutically relevant aspects in bone repair and regeneration, *Mater. Today*, 2015, 18(10), 573-589.
- [3] Lakhkar N.J., Lee I.-H., Kim H.-W., Salih V., Wall I.B., Knowles J.C., Bone formation controlled by biologically relevant inorganic ions: Role and controlled delivery from phosphate-based glasses, *Adv. Drug Deliv. Rev.*, 2013, 65(4), 405-420.
- [4] Knowles J.C., Phosphate based glasses for biomedical applications, *J. Mater. Chem.*, 2003, 13(10), 2395-2401.
- [5] Sezer N., Evis Z., Kayhan S.M., Tahmasebifar A, Koç M. Review of magnesium-based biomaterials and their applications, *J Magnes. and Alloys*, 2018, 6(1), 23-43.
- [6] Sharmin N., Rudd C.D., Structure, thermal properties, dissolution behaviour and biomedical applications of phosphate glasses and fibres: a review, *J Mater.Sci.*, 2017, 52(15), 8733-8760.
- [7] Abou-Neel E.A., Ahmed I, Blaker J.J., Bismarck A., Boccaccini A.R., Lewis M.P., Effect of iron on the surface, degradation and ion release properties of phosphate-based glass fibres, *Acta Biomater.*, 2005, 1(5), 553-563.
- [8] Abou-Neel E.A., Chrzanowski W., Knowles J.C., Biological performance of titania containing phosphate-based glasses for bone tissue engineering applications, *Mater. Sci. Eng. C*, 2014, 35, 307-313.
- [9] Sharmin N., Hasan M.S., Parsons A.J., Furniss D., Scotchford C.A., Ahmed I., Rudd C.R., Effect of Boron Addition on the Thermal, Degradation, and Cytocompatibility Properties of Phosphate-Based Glasses, *BioMed Res. Int.*, 2013, 2013, 12.
- [10] Balasubramanian P., Büttner T., Miguez P.V., Boccaccini A.R., Boron-containing bioactive glasses in bone and soft tissue engineering, *J. Eur. Ceram. Soc.*, 2018, 38(3), 855-869.
- [11] Li S., Lu Y., Qu Y., Xu Y., Ming L., Song Z., Influences of ZnO on the chemical durability and thermal stability of calcium iron phosphate glasses, *J. Non-Cryst. Solids.*, 2018, 498, 228-35.
- [12] Oueslati-Omrani R., Hamzaoui A.H., Chtourou R., M'Nif A., Structural, thermal and optical properties of phosphate glasses doped with SiO<sub>2</sub>, *J. Non-Cryst. Solids*, 2018, 481, 10-16.
- [13] Liu J., Zhu Y., Wang F., Liao Q., Zhu H., Deng Y., Zhu Y., Properties and structural features of iron sodium phosphate glasses containing neodymium oxide, *J. Non-Cryst.Solids*, 2018.
- [14] Wang Y., Zhu C., Parsons A., Rudd C.D., Ahmed I., Sharmin N., Effects of ZnO addition on thermal properties, degradation and biocompatibility of P45Mg24Ca16Na(15-x)Znx glasses, *Biomed. Glasses*, 2019, 53.
- [15] Rahaman M.N., Day D.E., Sonny B.B., Fu Q., Jung S.B., Bonewald L.F., Tompsia A.P., Bioactive glass in tissue engineering, *Acta Biomater.*, 2011, 7(6), 2355-2373.
- [16] Ahmed M., Effect of magnesium content on bioactivity of near invert phosphate-based glasses, *Int. J. App. Glass Sci.*, 2017, 8(4), 391-402.
- [17] Sharmin N., Gu F., Ahmed I., Parsons A.J., Compositional dependency on dissolution rate and cytocompatibility of phosphate-based glasses: Effect of B2O3 and Fe2O3 addition, *J. Tissue Eng.*, 2017, 8, 20-41.

- [18] Sharmin N., Hasan M.S., Rudd C.D., Boyd D., Werner-Zwanziger U., Ahmed I., Parsons A.J., Effect of boron oxide addition on the viscosity-temperature behaviour and structure of phosphate-based glasses. *J. biomed. mater. res. Part B, App. biomater.*, 2017, 105(4), 764-777.
- [19] Nielsen F.H., Studies on the relationship between boron and magnesium which possibly affects the formation and maintenance of bones, *Magnesium and trace elem.*, 1990, 9(2), 61-69.
- [20] Chapin R.E., Ku W.W., Kenney M.A., McCoy H., The effects of dietary boric acid on bone strength in rats, *Biol. trace elem. res.*, 1998, 66(1-3), 395-399.
- [21] Bunker B.C., Arnold G.W., Wilder J.A., Phosphate glass dissolution in aqueous solutions, *J. Non-Cryst. Solids*, 1984, 64(3), 291-316.
- [22] Carta D., Qiu D., Guerry P., Ahmed I., Abou-Neel E.A., Knowles J.C., Smith M.E., Newport R.J., The effect of composition on the structure of sodium borophosphate glasses, *J. Non-Cryst. Solids*, 2008, 354(31), 3671-3677.
- [23] Massera J., Shpotyuk Y., Sabatier F., Jouan T., Boussard-Plédel C., Roiland C., Bureau B., Petit L., Boetti N.G., Milanese D., Hupa L., Processing and characterization of novel borophosphate glasses and fibers for medical applications, *J. Non-Cryst. Solids*, 2015, 425, 52-60.
- [24] Donald I.W., Metcalfe B.L., Fong S.K., Gerrard L.A., The influence of Fe<sub>2</sub>O<sub>3</sub> and B<sub>2</sub>O<sub>3</sub> additions on the thermal properties, crystallization kinetics and durability of a sodium aluminum phosphate glass, *J. Non-Cryst. Solids*, 2006, 352(28), 2993-3001.
- [25] Baazm M., Soheyli E., Hekmatshoar M.H., Rostamzad A., Karami C.A.A., Preparation of quaternary boro-phosphate multifunctional glasses and their structural, optical, switching and antibacterial properties, *Ceram. Int.*, 2018, 44(8), 9414-9421.
- [26] Larink D., Eckert H., Reichert M., Martin S.W., Mixed Network Former Effect in Ion-Conducting Alkali Borophosphate Glasses: Structure/Property Correlations in the System [M<sub>2</sub>O]<sub>1/3</sub>[(B<sub>2</sub>O<sub>3</sub>)<sub>x</sub>(P<sub>2</sub>O<sub>5</sub>)<sub>1-x</sub>]<sub>2/3</sub> (M = Li, K, Cs), *The J. Phys. Chem. C.*, 2012, 116(50), 26162-26176.
- [27] Joseph K., Stennett M.C., Hyatt N.C., Asuvathraman R., Dube C.L., Gandy A.S., Iron phosphate glasses: Bulk properties and atomic scale structure, *J. Nucl. Mater.*, 2017, 494, 342-53.
- [28] Ahmed I., Collins C.A., Lewis M.P., Olsen I., Knowles J.C., Processing, characterisation and biocompatibility of iron-phosphate glass fibres for tissue engineering, *Biomater.*, 2004, 25(16), 3223-3232.
- [29] Saranti A., Koutselas I., Karakassides M.A., Bioactive glasses in the system CaO–B<sub>2</sub>O<sub>3</sub>–P<sub>2</sub>O<sub>5</sub>: Preparation, structural study and in vitro evaluation, *J. Non-Cryst. Solids*, 2006, 352(5), 390-398.
- [30] Pemberton J.E., Latifzadeh L., Fletcher J.P., Risbud S.H., Raman spectroscopy of calcium phosphate glasses with varying calcium oxide modifier concentrations, *Chem. of Mater.*, 1991, 3(1), 195-200.
- [31] Sharmin N., Hasan M.S., Parsons A.J., Rudd C.D., Ahmed I., Cytocompatibility, mechanical and dissolution properties of high strength boron and iron oxide phosphate glass fibre reinforced bioresorbable composites, *J. Mech. Behav. Biomed. Mater.*, 2016, 59, 41-56.
- [32] Zhu C., Ahmed I., Parsons A.J., Hossain K.M.Z., Rudd C.D., Liu X., Structural, thermal, in vitro degradation and cytocompatibility properties of P<sub>2</sub>O<sub>5</sub>-B<sub>2</sub>O<sub>3</sub>-CaO-MgO-Na<sub>2</sub>O-Fe<sub>2</sub>O<sub>3</sub> glasses, *J. Non-Cryst. Solids*, 2017, 77-85.
- [33] Vrouwenvelder W.C.A., Groot C.G., Groot K., Better histology and biochemistry for osteoblasts cultured on titanium-doped bioactive glass: Bioglass 45S5 compared with iron-, titanium-, fluorine- and boron-containing bioactive glasses, *Biomater.*, 1994, 15(2), 97-106.
- [34] Fu H., Fu Q., Zhou N., Huang W., Rahaman M.N., Wang D., Liu X., In vitro evaluation of borate-based bioactive glass scaffolds prepared by a polymer foam replication method, *Mater. Sci. Eng. C*, 2009, 29(7), 2275-2281.
- [35] Brown R.F., Rahaman M.N., Dwilewicz A.B., Huang W., Day D.E., Li Y., Bal B.S., Effect of borate glass composition on its conversion to hydroxyapatite and on the proliferation of MC3T3-E1 cells, *J. biomed. mater. res. Part A*, 2009, 88(2), 392-400.
- [36] Hasan M.S., Ahmed I., Parsons A.J., Walker G.S., Scotchford C.A., Material characterisation and cytocompatibility assessment of quinary phosphate glasses, *J. mater. sci. Mater. in med.*, 2012, 23(10), 2531-2541.
- [37] Uo M., Mizuno M., Kuboki Y., Makishima A., Watari F., Properties and cytotoxicity of water soluble Na<sub>2</sub>O–CaO–P<sub>2</sub>O<sub>5</sub> glasses, *Biomater.*, 1998, 19(24), 2277-2284.
- [38] Mancuso E., Bretcanu O.A., Marshall M., Birch M.A., McCaskie A.W., Dalgarno K.W., Novel bioglasses for bone tissue repair and regeneration: Effect of glass design on sintering ability, ion release and biocompatibility, *Mater. & Design*, 2017, 129, 239-248.
- [39] Rajkumar G., Dhivya V., Mahalaxmi S., Rajkumar K., Sathishkumar G.K., Karpagam R., Influence of fluoride for enhancing bioactivity onto phosphate based glasses, *J. Non-Cryst. Solids*, 2018, 493, 108-118.